Partially Buried Microcolumns for Micro Gas Analyzers

ARTICLE *in* ANALYTICAL CHEMISTRY · MAY 2009

Impact Factor: 5.64 · DOI: 10.1021/ac8027382 · Source: PubMed

4 AUTHORS, INCLUDING:

Adarsh D Radadia
Louisiana Tech University
25 PUBLICATIONS **270** CITATIONS

SEE PROFILE

Anal. Chem. **2009,** *81,* 3471–3477

Partially Buried Microcolumns for Micro Gas Analyzers

Adarsh D. Radadia,*,† Robert D. Morgan,† Richard I. Masel,*,† and Mark A. Shannon‡

Department of Chemical and Biomolecular Engineering and Department of Mechanical Science and Engineering, University of Illinois at Urbana−Champaign, Department of Mechanical Science and Engineering, University of Illinois at Urbana−Champaign, Urbana, Illinois 61801-2302

This article demonstrates the feasibility of making a partially buried micro gas chromatography (μ-GC) column with a rounded channel wall profile, which enables coating the stationary phase more uniformly and shows better separation characteristics than a square deep reactive ion etched (DRIE) wall profile. A buried structure fabrication method was adapted to fabricate 34 cm long, 165 μm wide, and 65 μm deep partially buried microcolumns, which had a unique rounded microcolumn wall profile similar to that of a flattened circular tube. The separation characteristics were compared to that of a 34 cm long, 100 μm × 100 μm square DRIE microcolumn, which had a similar hydraulic diameter. Minimum height equivalent to a theoretical plate (HETP) and reduced HETP of 0.39 mm and 6.02, respectively, with a retention factor of 6.3 were obtained on the coated partially buried microcolumn compared to 0.66 mm and 6.73, respectively, on the coated square DRIE microcolumn with a similar retention factor. The partially buried microcolumn was found to perform closer to the theoretical approximation and this could be attributed to the uniform phase deposition in the partially buried microcolumn compared to the square DRIE microcolumn. A 10 component mix was separated on the partially buried microcolumn in 3.8 s with the maximum peak width at half-height equal to 0.2 s, while a similar mix separated at higher pressure and temperature conditions on the square DRIE microcolumn in 4.6 s. The rounded corners allowed depositing thinner stationary phase, which was reflected in the faster elution of *n*-C_{12} on the partially buried microcolumn compared to the square DRIE microcolumn. The better performance of the partially buried microcolumn may be attributed to either the rounded channel wall profile, the clean channel structures produced by the fabrication process, or the double-etched wall profile, which lowers the Taylor-Aris dispersion.

Micro gas chromatography (μGC) has been an attractive solution for portable detection of several classes of compounds including toxic chemicals, explosives, disease markers, and other analytes. Several advances have been reported in the development of μGC components including pre-concentrators,[1−7] columns,[8−26] detectors,[27−32] valves,[33] and pumps. Efforts showing some integra-

(1) Chan, H. K. L. A microfabricated preconcentrator for sample extraction and injection in microscale gas chromatography. PhD Thesis, University of Michigan, Ann Arbor, MI, 2006.
(2) Kim, M.; Mitra, S. *J. Chromatogr., A* **2003**, *996*, 1–11.
(3) Lewis, P. R.; Manginell, R. P.; Adkins, D. R.; Kottenstette, R. J.; Wheeler, D. R.; Sokolowski, S. S.; Trudell, D. E.; Byrnes, J. E.; Okandan, M.; Bauer, J. M.; Manley, R. G.; Frye-Mason, G. C. *IEEE Sens. J.* **2006**, *6*, 784–795.
(4) Ni, Z.; Jerrell, J. P.; Cadwallader, K. R.; Masel, R. I. *Anal. Chem.* **2007**, *79*, 1290–1293.
(5) Tang, Y., Yeom, J., Bae, B., Masel, R. I., Shannon, M. A. *Proceedings of Ninth International Conference on Miniaturized Systems for Chemistry and Life Sciences - μTAS '05*, Boston, U.S.A. Oct. 9−13, 2005.
(6) Tian, W.-C.; Pang, S. W.; Lu, C.-J.; Zellers, E. T. *J. Microelectromech. Syst.* **2003**, *12*, 264–272.
(7) Yeom, J.; Oh, I.; Field, C.; Radadia, A.; Ni, Z.; Bae, B.; Han, J.; Masel, R. I.; Shannon, M. A *J. Microelectromech. Syst.* **2008**, 232–235.
(8) Agah, M.; Lambertus, G. R.; Sacks, R.; Wise, K. *J. Microelectromech. Syst.* **2006**, *15*, 1371–1378.
(9) Agah, M.; Wise, K. D. *J. Microelectromech. Syst.* **2007**, *16*, 853–860.
(10) Bhushan, A.; Yemane, D.; Overton, E. B.; Goettert, J.; Murphy, M. C. *J. Microelectromech. Syst.* **2007**, *16*, 383–393.
(11) Bhushan, A.; Yemane, D.; Trudell, D.; Overton, E. B.; Goettert, J. *Microsys. Technol.* **2007**, *13*, 361–368.
(12) Hannoe, S.; Sugimoto, I.; Yanagisawa, K.; Kuwano, H. *Transducers 97, International Conference on Solid-State Sensors and Actuators*, Chicago, June 16−19, 1997; Vol. 1, pp 515−518.
(13) Lambertus, G.; Elstro, A.; Sensenig, K.; Potkay, J.; Agah, M.; Scheuering, S.; Wise, K.; Dorman, F.; Sacks, R. *Anal. Chem.* **2004**, *76*, 2629–2637.
(14) Lambertus, G. R.; Fix, C. S.; Reidy, S. M.; Miller, R. A.; Wheeler, D.; Nazarov, E.; Sacks, R. *Anal. Chem.* **2005**, *77*, 7563–7571.
(15) Lehmann, U. (SLS Micro Technology G.m.b.H., Germany). WO 2006042727, 2006.
(16) Lehmann, U.; Krusemark, O.; Muller, J. *Micro Total Analysis Systems 2000; Proceedings of the micro TAS Symposium, 4th*, Enschede, Netherlands, May 14−18, 2000; pp 167−170.
(17) Matzke, C. M.; Kottenstette, R. J.; Casalnuovo, S. A.; Frye-Mason, G. C.; Hudson, M. L.; Sasaki, D. Y.; Manginell, R. P.; Wong, C. C. *Proc. SPIE* **1998**, *3511*, 262–268.
(18) Noh, H. S.; Hesketh, P. J.; Frye-Mason, G. C. *J. Microelectromech. Syst.* **2002**, *11*, 718–725.
(19) Radadia, A. D., Shannon, M. A., Masel, R. I. *Proceedings of the 15th International Conference on Solid State Sensors, Actuators and Microsystems - Transducers*, Lyon, France, June 10−15, 2007; p 1343.
(20) Radadia, A. D.; Masel, R. I.; Shannon, M. A.; Jerrell, J. P.; Cadwallader, K. R. *Anal. Chem.* **2008**, *80*, 4087–4094.
(21) Radadia, A. D.; Masel, R. I.; Strano, M. S.; Shannon, M. A.; Cadwallader, K. R. In *AICHE Annual Meeting*, Cincinnati, OH, 2005.
(22) Reidy, S.; George, D.; Agah, M.; Sacks, R. *Anal. Chem.* **2007**, *79*, 2911–2917.
(23) Reidy, S.; Lambertus, G.; Reece, J.; Sacks, R. *Anal. Chem.* **2006**, *78*, 2623–2630.
(24) Stadermann, M.; McBrady, A. D.; Dick, B.; Reid, V. R.; Noy, A.; Synovec, R. E.; Bakajin, O. *Anal. Chem.* **2006**, *78*, 5639–5644.
(25) Stuermann, J.; Lang, W.; Benecke, W.; Zampoli, S.; Elmi, I. *Chem. Sens.* **2004**, *20*, 824–825.

* To whom correspondence should be addressed. E-mail: r-masel@illinois.edu.
† Department of Chemical and Biomolecular Engineering.
‡ Department of Mechanical Science and Engineering.

10.1021/ac8027382 CCC: $40.75 © 2009 American Chemical Society
Published on Web 04/07/2009

tion between components have also been reported.[34−40] Microfabricated silicon columns are attractive because (1) lower dead volume arises when integrating micromachined components and (2) silicon has better thermal properties, that is, (a) reduced heating and cooling times (in practical situation $Bi_{Si} = 0.011$, $Bi_{glass} = 1.1$), (b) lower power consumption (thermal mass density, $\rho_{Si}C_{p,Si} \sim 0.75\rho_{glass}C_{p,glass}$), and (c) a more even temperature distribution (thermal diffusivity, $\alpha_{Si} = 0.8$, $\alpha_{glass} = 0.0056$ cm^2/s).

Currently there are no design guidelines for column miniaturization. In particular, it is not known what wall profile a microcolumn should have for a better chromatographic performance. Early attempts used trapezoidal wall profiles, which are obtained using potassium hydroxide (KOH) etching.[35,38,39,41] Although KOH etching is a relatively easy fabrication method, the resulting channel profile is related to the silicon crystal planes and hence limits the column structures that can be fabricated. To overcome this limitation, hydrofluoric acid-nitric acid (HNA) based isotropic etching for silicon, and hydrofluoric acid (HF) based iso-etching for glass was used to create circular channels by aligning and bonding two isotropically etched substrates with semicircular channels.[12,26,40] In this case, the alignment process is an equipment intensive process and typical alignment accuracies are around 3 to 5 μm, which is a very high degree of misalignment compared to the typical stationary phase thickness (50−200 nm). Stationary phase deposition in such a microcolumn creates pooling of the phase in the misaligned structures. High aspect ratio rectangular columns are attractive for higher flow rate and sample capacity, although rectangular columns do not theoretically provide better separation characteristics compared to circular columns.[42−47] Sandia National Laboratory researchers first demonstrated the use of high aspect ratio channels as microcolumns for gas chromatography.[17] High aspect ratio microcolumns were made using deep reactive ion etching (DRIE) of microchannels in silicon followed by its capping with a Pyrex cover via anodic bonding. Currently researchers at various institutions have adopted the DRIE method to produce microcolumns. The gas chromatography performance is typically reported in terms of Golay plots, which are plots of height equivalent to a theoretical plate (HETP) versus the average carrier gas velocity. Theoretically, the HETP of a uniformly coated DRIE microcolumn can be predicted using

$$\mathrm{HETP} = \frac{B}{u} + C{\cdot}u + D{\cdot}u^2 \tag{1}$$

where u is the average carrier gas velocity, and B, C, and D are coefficients of the molecular diffusion driven band broadening term, respectively. the resistance to mass transfer driven band broadening term, and the extra-column band broadening term, respectively. The mass transfer driven band broadening term coefficient is a sum of two terms, each term corresponding to the mass transfer resistance in the mobile phase and the stationary phase. Typically, the stationary phase related term is ignored as it is negligible compared to the mobile phase related term. These coefficients can be estimated using

$$B = 2{\cdot}D_g \tag{2}$$

$$C = \frac{A' + B'{\cdot}k + C'{\cdot}k^2}{96(1+k)^2}\frac{d^2}{D_g} \tag{3}$$

where D_g is the molecular diffusivity of the retained molecule in the carrier gas, k is the retention factor, and d is the critical dimension of the microcolumn. The retention factor can be calculated experimentally using

$$k = \frac{t_R - t_M}{t_M} \tag{4}$$

where t_R and t_M are the retention times of the retained and non-retained (methane) molecules. Many solutions for the A', B', and C' exists.[42−45,47] Recently Liang et al. showed that coefficients A', B', and C' can be calculated with less than ±1.5% error using[43]

$$A' = 0.9143\left(1 - \frac{1.354 - R}{0.7609{\cdot}R^2 - 0.8973{\cdot}R + 1.734}\right) \tag{5}$$

$$B' = 8.229\left(1 - \frac{1}{0.9993{\cdot}R^2 - 0.2869{\cdot}R + 1.098}\right) \tag{6}$$

$$C' = 23.31\left(1 - \frac{1}{0.4878{\cdot}R + 0.8228}\right) \tag{7}$$

where R is the aspect ratio (width/height) of the microcolumn. For a 100 μm square DRIE microcolumn, assuming values for D_g, D, and k as 30 mm^2/s, 10^{-6} s^2/mm, and 6, respectively, a minimum HETP value of 0.3 mm can be predicted theoretically.

However, the DRIE microcolumns have sharp corners and are not suitable for uniform phase deposition. The DRIE microcol-

(26) Yu, C. (The Regents of the University of California, USA) WO 2000058723, 2000.
(27) Bessoth, F. G.; Naji, O. P.; Eijkel, J. C. T.; Manz, A. *J. Anal. At. Spectrom.* **2002**, *17*, 794–799.
(28) Cruz, D.; Chang, J. P.; Showalter, S. K.; Gelbard, F.; Manginell, R. P.; Blain, M. G. *Sens. Actuators, B* **2007**, *B121*, 414–422.
(29) Kendler, S.; Reidy, S. M.; Lambertus, G. R.; Sacks, R. D. *Anal. Chem.* **2006**, *78*, 6765–6773.
(30) Lee, C. Y.; Sharma, R.; Radadia, A. D.; Masel, R. I.; Strano, M. S. *Angew. Chem., Int. Ed.* **2008**, *47*, 5018–5021.
(31) Oh, I.; Masel, R. I. *Electrochem. Solid-State Lett.* **2007**, *10*, J19−J22.
(32) Schmidt, H.; Tadjimukhamedov, F.; Mohrenz, I. V.; Smith, G. B.; Eiceman, G. A. *Anal. Chem.* **2004**, *76*, 5208–5217.
(33) Bae, B.; Han, J.; Masel, R. I.; Shannon, M. A. *J. Microelectromech. Syst.* **2007**, *16*, 1461–1471.
(34) Dziuban, J. A.; Mroz, J.; Szczygielska, M.; Malachowski, M.; Gorecka-Drzazga, A.; Walczak, R.; Bula, W.; Zalewski, D.; Nieradko, L.; Lysko, J.; Koszur, J.; Kowalski, P. *Sens. Actuators, A* **2004**, *A115*, 318–330.
(35) Kolesar, E. S., Jr.; Reston, R. R. *J. Microelectromech. Syst.* **1994**, *3*, 147–154.
(36) Lorenzelli, L.; Benvenuto, A.; Adami, A.; Guarnieri, V.; Margesin, B.; Mulloni, V.; Vincenzi, D. *Biosens. Bioelectron.* **2005**, *20*, 1968–1976.
(37) Lu, C. J.; Steinecker, W. H.; Tian, W. C.; Oborny, M. C.; Nichols, J. M.; Agah, M.; Potkay, J. A.; Chan, H. K. L.; Driscoll, J.; Sacks, R. D.; Wise, K. D.; Pang, S. W.; Zellers, E. T. *Lab Chip* **2005**, *5*, 1123–1131.
(38) Reston, R. R.; Kolesar, E. S., Jr. *J. Microelectromech. Syst.* **1994**, *3*, 134–146.
(39) Terry, S. C.; Jerman, J. H.; Angell, J. B. *IEEE Trans. Electron Devices* **1979**, *ED-26*, 1880–1886.
(40) Wiranto, G.; Samaan, N. D.; Mulcahy, D. E.; Davey, D. E. *Proc. SPIE* **1997**, *3242*, 59–64.
(41) Saadat, S.; Terry, S. C. *Am. Lab.* **1984**, *16* (90), 9294, 96, 98−99, 101.
(42) Poppe, H. *J. Chromatogr. A* **2002**, *948*, 3–17.
(43) Liang, D.; Peng, Q.; Mitchelson, K.; Guan, X. S.; Xing, W. L.; Cheng, J. *Lab Chip* **2007**, *7*, 1062–1073.
(44) Spangler, G. E. *Anal. Chem.* **2006**, *78*, 5205–5207.
(45) Spangler, G. E. *J. Microcol. Sep.* **2001**, *13*, 285–292.
(46) Spangler, G. E. *Anal. Chem.* **1998**, *70*, 4805–4816.
(47) Ahn, H.; Brandani, S. *AIChe J.* **2005**, *51*, 1980–1990.

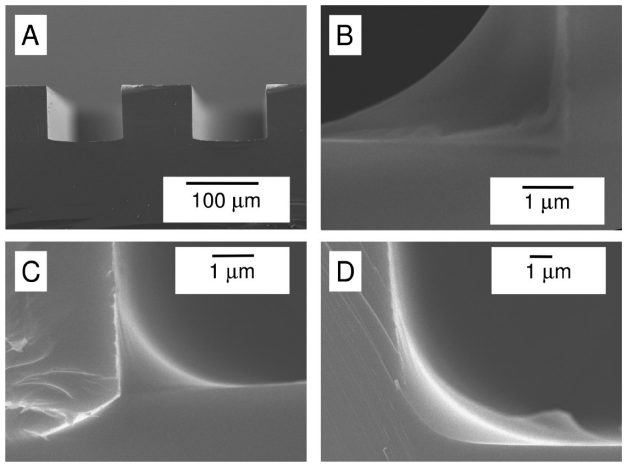

Figure 1. SEM images showing the 100 μm × 100 μm square cross-section of a square DRIE silicon-Pyrex microcolumn similar to previously reported [19−21] (A); stationary phase pooling in the sharp corners of a dynamically coated (B), and a statically coated (C) square DRIE microcolumn; and stationary phase deposited in a rounded corner of a dynamically coated microcolumn treated with the corner rounding treatment of SF_6 RIE after DRIE (D).

umns show notably lower performance compared to the conventional fused silica columns. Conventionally GC columns are coated by either a dynamic method or a static method. In dynamic coating a plug of stationary phase solution is driven through the column, whereas in static coating the columns are filled up with the coating solution and the solvent is evaporated by applying vacuum. Figure 1 shows scanning electron microscope (SEM) images from the coating experiments performed on 34 cm long, 100 μm × 100 μm DRIE microcolumns. Figure 1A shows the 100 μm square channel profile of a DRIE microcolumn, which when capped with Pyrex glass results in four sharp corners. Figure 1B and 1C show the stationary phase pooling that occurs when the DRIE microcolumns were coated dynamically and statically, respectively. The capillary force responsible for the pooling can be reduced by rounding the square corners using an isotropic etching processes like SF_6 reactive ion etching (RIE) or silicon anodization method following the DRIE process, which we have previously proposed.[19] Figure 1D shows comparatively reduced phase pooling at the rounded corners, which were formed by a short SF_6 RIE after the DRIE step. However, the process can only be applied to two out of the four corners of the DRIE silicon-Pyrex channel, and the corner rounding process does not produce satisfactory phase uniformity. Panels A and B of Figure 2 show the previously reported Golay plots and an example separation of an 8 component mix on a coated DRIE microcolumn. Notice the minimum obtained HETP value on the square DRIE microcolumn is 0.66 mm (compared to 0.3 theoretically predicted) and the maximum peak width at half-maximum in the chromatogram is 0.33 s.

(48) de Boer, M. J.; Tjerkstra, R. W.; Berenschot, J. W.; Jansen, H. V.; Burger, C. J.; Gardeniers, J. G. E.; Elwenspoek, M.; van den Berg, A. *J. Microelectromech. Syst.* **2000**, *9*, 94–103.
(49) Tjerkstra, R. W.; deBeer, M.; Berenschot, E.; Gardeniers, J. G. E.; vandenBerg, A.; Elwenspoek, M. C. *Electrochim. Acta* **1997**, *42*, 3399–3406.
(50) Tjerkstra, R. W. Isotropic etching of silicon in fluoride containing solutions as a tool for micromachining. Ph.D. Thesis, University of Twente, Enschede, The Netherlands, 1999.

The stationary phase pooling related issues can be solved by fabricating completely rounded microchannels without the need for high accuracy alignment processes. We found that Tjerkstra et al. proposed such a solution for chromatography called the buried channel technology (BCT), where the channels were completely enclosed inside the silicon substrate;[48−50] however, no results were reported for the buried microcolumns. Recently Agah et al. adopted the buried channel fabrication technique to make semicircular silicon-oxynitride (SiON) μGC columns aiming to make low thermal mass microcolumns for rapid temperature programming.[9] However, the separation performance was not comparative to the commercial columns, and no experimental Golay plot data was reported.

The objective of the work described in this article is to report the fabrication of partially buried microcolumns and that separation on microcolumns can be improved, especially at high velocities (greater than optimum velocity) by changing the column wall profile from square to a rounded one. A flattened circular column wall profile was accomplished using the partially buried channel fabrication method, a variation of the BCT. The wall profile obtained in this paper allowed uniform deposition of stationary phase compared to square DRIE microcolumns. The paper compares the Golay plots and separation results of coated partially buried microcolumns to coated DRIE microcolumns with similar hydraulic diameter.

EXPERIMENTAL SECTION

Microfabrication. Figure 3 is a brief schematic presentation of the fabrication sequence that was followed to fabricate partially buried microcolumns. The wafer processing steps included column fabrication (Figure 3, steps A−G) followed by fabrication of fluidic access holes (Figure 3, steps H and I) and capping of the microchannels (Figure 3, step J). Microfabrication started with a double side polished silicon wafer (4″ diameter, 250 μm thick, 5−20 ohms-cm p-type, Silicon Quest International), which were first oxidized to grow a 1.7 μm thick wet oxide on the surface (Figure 3A). Shipley SPR220-7 photoresist was spin coated on one side of the wafer at 3000 rpm. Photolithography was performed to obtain an image of 24 dies each containing 100 μm wide and 34 cm long serpentine channels (Figure 3B). The patterned photoresist was baked at 90 °C for 30 min to withstand the subsequent reactive ion etching (RIE) steps. The channel pattern was transferred to the oxide layer using CF_4 RIE (also known as Freon RIE). Then exposed silicon surface in the channel region was etched 11 μm anisotropically using DRIE (Figure 3C). The DRIE was followed by a 4 min SF_6 isotropic RIE process to remove defects and produce cleaner column structures. The photoresist was removed from the wafer using acetone before depositing 0.3 μm thick silicon dioxide (SiO_2) with plasma enhanced chemical vapor deposition (PECVD) (Figure 3D). DRIE was performed for 20 min to etch the PECVD oxide deposited at the bottom of the channels. The latter step etched the PECVD oxide all over the wafer except at the channel sidewalls (Figure 3E). Isotropic etching of the wafer with SF_6 RIE for 25 min was used to create the partially buried channel structure (Figure 3F). The wafer was then exposed to buffered oxide etch solution (BOE) to etch all the oxide. A special wall smoothening step was introduced to reduce the channel wall roughness. The smoothing process involved growing 1.7 μm thick

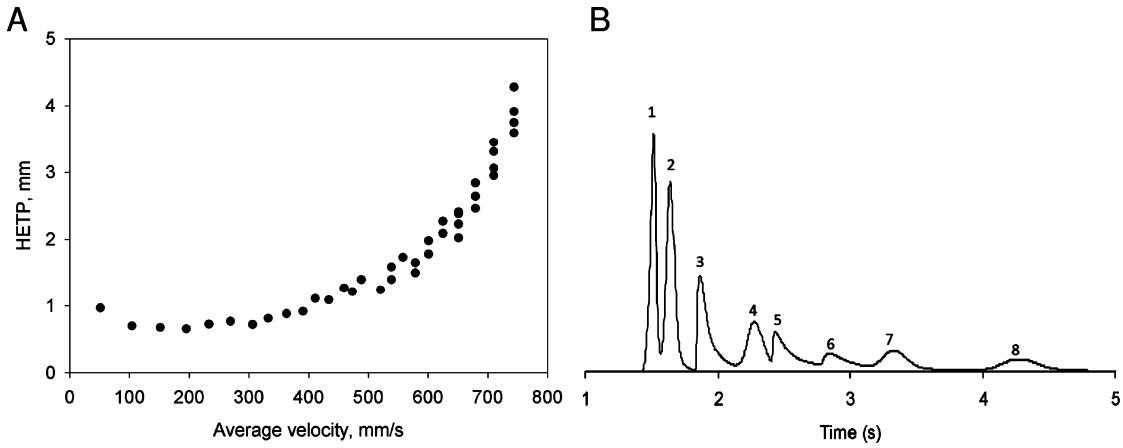

Figure 2. (A) Golay plot for a 34 cm long, 100 μm square DRIE silicon-Pyrex microcolumns measured using methane elution time for velocity measurements and *n*-C_9 elution time and peak width for HETP calculations. Temperature of the microcolumn was adjusted to obtain a retention factor of 6 for *n*-C_9 at 25 cm/s of helium flow. (B) Example separation of diethyl ether (1), toluene (2), dimethyl methyl phosphonate (3), diethyl methyl phosphonate (4), *n*-octanol (5), diisopropyl methyl phosphonate (6), 1,6-dichlorohexane (7), and dodecane (8) mix obtained on a square DRIE silicon-Pyrex microcolumn; 1 μL of headspace was injected with a 100:1 split; injector temperature 250 °C, inlet pressure of 25 psi, and oven temperature ramped from 90 to 98 at 120 °C/min. Hydrogen was used as the carrier gas.

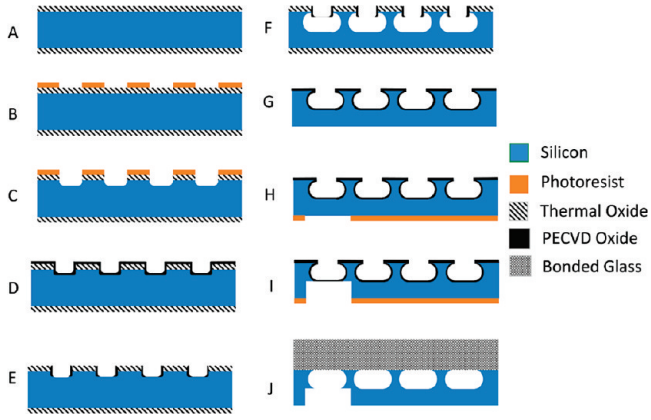

Figure 3. Brief schematic outline of the fabrication process used to create partially buried microcolumns. The fabrication steps include 1.7 μm wet oxide growth (A), channel patterning using photolithography (B), CF_4 RIE, DRIE, SF_6 RIE (C), photoresist strip, 0.3 μm PECVD oxide deposition (D), DRIE (E), SF_6 RIE (F), BOE etch, 1.7 μm wet oxide growth, BOE etch, 0.25 μm thick PECVD oxide deposition (G), access hole patterning using photolithography (H), DRIE of access holes (I), cleaning and anodic bonding (J). More detailed process information is provided in the text.

wet oxide followed by its etching with BOE. The channel side of the wafer was then protected from being damaged in the further processing steps by depositing a 0.25 μm thick PECVD oxide layer (Figure G).

The non-processed side of the silicon wafer was spin coated with SPR220-7 at 3000 rpm and access holes corresponding to the channels on the first side were patterned using aligned photolithography (Figure 3H). The photoresist was baked at 90 °C for 30 min to help it withstand the following DRIE step. DRIE was performed on the patterned side to form the access holes (Figure 3I). The wafer was also diced in the latter step. The resulting columns dies were cleaned with acetone to strip the photoresist layer, followed by a BOE rinse to remove the PECVD oxide protecting the channel side of the wafer. A standard clean 1 (SC-1) at 73 °C was performed to clean the surface. Pyrex 7740 glass pieces of the size of silicon die were cut out from 4″ wafers using a laser machine and cleaned by an SC-1 clean procedure. Silicon channels were anodically sealed with the cleaned Pyrex glass at 400 °C with 900 V bias (Figure 3J).

Deactivation. Organosilicon hydride passivation using phenyltris(dimethylsiloxy)silane (Ah3P) (Gelest, SIP6826) was performed as previously reported.[20] The passivation was performed by dynamically coating the surface with one column length plug of neat reagent. A brass reservoir manifold containing the solution was attached on one of the microcolumn access ports, and the plug was pulled using a 660.4 mmHg vacuum at the second access port. After the liquid plug exited the microcolumn, the column was heat-treated in a vacuum annealer (300 μm Hg) at a rate of 8 °C min^{-1} to 375 °C and held at the final temperature for 4 h. The microcolumn was cooled to room temperature before exposing to the atmosphere.

Stationary Phase Coating. A 5% polar stationary phase, OV-5 vinyl gum obtained from Ohio Valley Specialty Company (Marietta, Ohio) was used as the stationary phase. The coating solutions were prepared in hexamethyldisilazane treated 12 × 32 vials obtained from Alltech (#72670). The stationary phase (in the range of 0.05−0.07 g) was transferred to a vial, and 0.2 μm-filtered pentane was injected into the capped vial using a syringe to produce a 1% (w/v) coating solution. The phase was dissolved by sonicating the vial for 20 min. Dicumyl peroxide (DCP) (Sigma Aldrich, >99%) in the form of freshly prepared 2% (w/v) toluene solution was added to the coating solution to achieve a DCP concentration of 1% (w/w) of the stationary phase.

Each end of a microcolumn was connected to a 30 cm long fused silica capillary (200 μm O.D., 100 μm I.D., Polymicro Technologies) using Nanoports (Upchurch Scientific, N-125S). The coating solution was introduced through one of the fused silica capillaries until four drops of the coating solution was seen to leave through other end of the setup. The microcolumn was attached to a GC inlet using one of the fused silica capillaries, and the coating solution was driven out using 0.8 psi helium pressure. When the coating solution exited the free capillary end, the solvent from the coated stationary phase was removed by passing helium at 40 psi inlet pressure for 2 min. Subsequently,

the helium pressure was reduced to 0.8 psi, and the stationary phase was cross-linked and conditioned by heating the microcolumn to 160 °C overnight.

Post-coating Treatment. Post-coating pinacolyl methylphosphonic acid (PMP) deactivation treatment was performed as previously reported. [20] The PMP treatment was performed on a conventional GC at 110 °C by injecting 1 μL of liquid PMP in the splitless mode (injector temperature of 250 °C) with a helium flow at 40 psi followed by a stabilizing time of 1 h with the helium flowing. The microcolumn was reconditioned at 200 °C with 40 psi inlet pressure for 1 h. The completion of the reconditioning process was checked with the presence of a stable FID baseline. The connecting fused silica capillaries were replaced with deactivated guard capillaries for testing.

Partially Buried Microcolumn Testing. An Agilent 6893N GC/FID-MS equipped with 7683B autosampler was used for all the separations. Packaged microcolumns were placed in the GC oven for testing and connected to the split inlet and the detector using Restek deactivated guard capillaries (100 μm I.D., 200 μm O.D., and 30 cm long, IP deactivated). Helium was used as the carrier gas in this paper. The injector temperature was held at 250 °C. A flame ionization detector was used at 250 °C, the time constant was at 200 Hz. Test mixtures were prepared using puriss-grade chemicals (GC standards) from Aldrich (Milwaukee, WI).

(a) Column Efficiency Measurements. The column efficiency was evaluated by calculating the effective HETP as a function of average carrier gas velocity. The average carrier gas velocity was estimated using methane injections and *n*-decane elution characteristics were used for calculating HETP. The sample vial was prepared by transferring 0.2 μL of liquid *n*-decane into the vial and then injecting 40 μL of methane into the vial. One microliter of headspace vapor was injected with a split of 5000:1; the partially buried microcolumns were held at 44 °C in the GC oven to achieve a retention factor of 6.3 at 25 cm/s. The inlet pressure of the carrier gas was varied from 2 to 34 psi. The resulting chromatograms were analyzed using MSD Chemstation software to calculate the retention time and peak width at half-maximum. The HETP values were calculated using

$$\mathrm{HETP} = \frac{w_h^2 \cdot L}{5.54 \cdot t^2} \tag{8}$$

where t is the retention time of *n*-decane (t_R) minus the retention time of methane (t_M), L is the length of microcolumn and w_h is the full width at half-maximum of the *n*-decane peak. Equations 1−7 were used to theoretically predict HETP for square microcolumns. In the absence of a theoretical model to predict HETP for columns of arbitrary cross-section, theoretical predictions for a rectangular microcolumn with the same width and depth as the partially buried microcolumn were used to compare experimental HETP results of the partially buried microcolumn. Because of the difference in critical dimensions of the partially buried microcolumns and the previously demonstrated square DRIE microcolumns, reduced HETP (h) values were used to compare the difference between the theoretical and experimental data. Reduced HETP values were calculated by dividing the HETP value with the value for the critical dimension of the respective microcolumn. The effect of turns on dispersion in microcolumns has not been accounted for in the theoretical predictions.

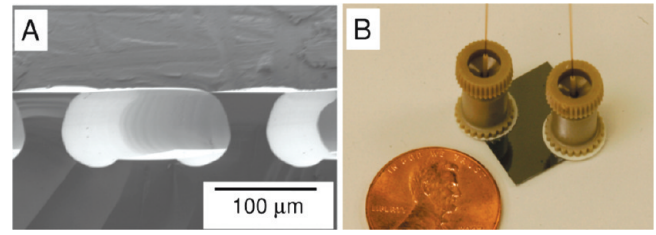

Figure 4. (A) SEM image showing the 165 μm wide and 65 μm deep cross-section of a partially buried microcolumn. (B) Photograph showing a 1.4 cm square microcolumn die fabricated in this paper packaged with Nanoport fittings connecting the access holes on the die to the fused silica capillaries.

(b) Separation Test. A 10 component mix similar to the one demonstrated in Figure 1B was prepared to compare separation capability of the partially buried microcolumn to that of the square DRIE microcolumn. The mix was formulated by transferring 0.2 μL of dimethyl methylphosphonate (DMMP), diethyl methylphosphonate (DEMP), diisopropyl methylphosphonate (DIMP), and 1,6-dichlorohexane (DCH); the vial was capped and 300 μL headspace of toluene, diethyl ether, and *n*-C_9 to *n*-C_{12} each was injected into the vial. The separation test was performed by injecting 1 μL vial headspace with a split of 3000:1 into the microcolumn, which was held at 85 °C, and the carrier gas inlet pressure was held at 13.5 psi.

RESULTS

Microfabrication. Figure 4A shows a SEM image of the partially buried microcolumn fabricated in this paper. The resultant channels were found to be 165 μm wide and 65 μm deep. The hydraulic diameter of the channel was calculated to be 107 μm. The SEM image shows that the here proposed microcolumn fabrication results in a partially buried isotropic wall profile. The capping of the partially buried channels with a flat Pyrex lid would result in a cavity that looks like two channels with iso-etch wall profile align bonded together; the top channel having a single-etched wall profile and bottom channel having a single-etched wall profile with a rectangular ridge, similar to the double-etched isotropic profile as defined by Dutta and Leighton.[51−55] The walls were found to be smoother compared to the DRIE walls, which are typically scalloped. The scallop-free walls minimize pooling of the stationary phase on the walls. No micrograss, constrictions, or fabrication defects were observed with the SEM in the channels inspected so far. Figure 4B shows the 34 cm long microcolumn die sizing 1.4 cm × 1.4 cm, which was connected to the fused silica capillaries via Nanoports.

Partially Buried Microcolumn Performance. *(a) Column Efficiency Measurements.* Figure 5a shows the plot of HETP versus average carrier gas velocity obtained on a coated partially buried microcolumn in comparison to the experimental results from square DRIE microcolumn. Figure 5a also shows the theoretically predicted values for a 100 μm square microcolumn and 165 μm wide × 65 μm deep rectangular microcolumn. Minimum HETP

(51) Dutta, D.; Leighton, D. T. *Anal. Chem.* **2001**, *73*, 504–513.
(52) Dutta, D.; Leighton, D. T. *Anal. Chem.* **2002**, *74*, 1007–1016.
(53) Dutta, D.; Leighton, D. T. *Anal. Chem.* **2003**, *75*, 3352–3359.
(54) Dutta, D.; Leighton, D. T. *Anal. Chem.* **2003**, *75*, 57–70.
(55) Dutta, D.; Ramachandran, A.; Leighton, D. T. *Microfluid. Nanofluid.* **2006**, *2*, 275–290.

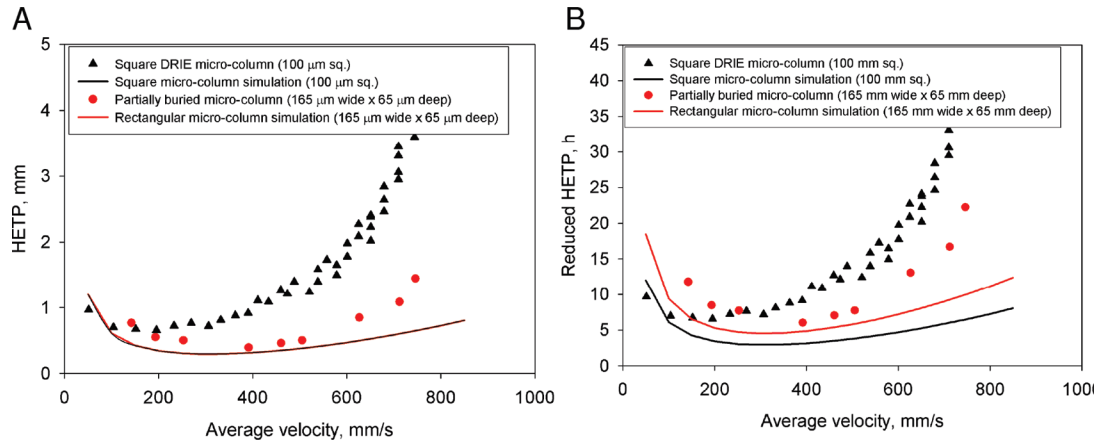

Figure 5. Golay plot (a) and reduced HETP plot (b) for a 34 cm long, 165 μm wide $\times$ 65 μm deep partially buried microcolumns in comparison to a 100 μm square DRIE microcolumn. The data for the square DRIE column is retrieved from Figure 2A. Reduced HETP plots were calculated using critical dimensions of 65 and 100 μm for the partially buried column and square DRIE microcolumn, respectively. The experimental plot for the partially buried microcolumn is generated using methane elution time for velocity measurements and *n*-C_{10} elution time and peak width for HETP calculations. Temperature of the microcolumn was adjusted to obtain a retention factor of 6.3 for *n*-C_{10} at 25 cm/s of helium flow. Theoretical data (simulation) was calculated using eqs 1−7, assuming values of D_g, D, and k as 30 mm^2/s, 10^{-6} s^2/mm, and 6, respectively.

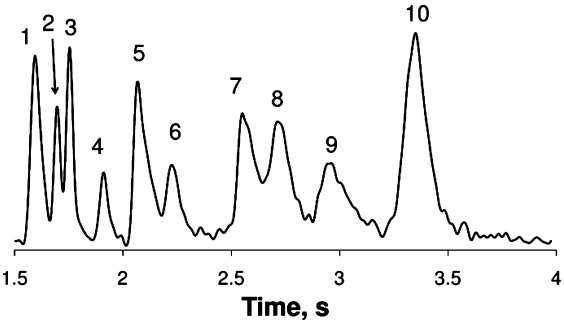

Figure 6. Example separation of diethyl ether (1), toluene (2), *n*-C_9 (3), *n*-C_{10} (4), dimethyl methyl phosphonate (5), *n*-C_{11} (6), diethyl methyl phosphonate (7), diisopropyl methyl phosphonate (8), *n*-C_{12} (9), and 1,6-dichlorohexane (10) mix obtained on a partially buried microcolumn; 1 μL of headspace was injected with a 3000:1 split; injector temperature 250 °C, inlet pressure of 13.5 psi, and oven temperature held at 85 °C. Helium was used as the carrier gas.

on the partially buried microcolumn was found to be 0.39 mm, and the corresponding average velocity (optimum gas velocity) was found to be 40 cm/s. The theoretical prediction for a 165 μm wide $\times$ 65 μm deep rectangular microcolumn was found to be 0.29 mm. Figure 5b shows the plot of reduced HETP versus the average carrier gas velocity. The experimental minimum reduced HETP values for partially buried microcolumn and square DRIE microcolumn were found to be 6.02 and 6.73, respectively, as compared to theoretical predictions of 4.53 and 2.95, respectively.

(b) Separation Test. Figure 6 shows that it is possible to separate the 10 compound mix on the coated partially buried microcolumn within 3.6 s when the carrier gas inlet pressure and oven temperature were held at 13.5 psi and 85 °C, respectively. The chromatogram shows a maximum peak width at half-maximum of 0.2 s. The peaks elute in a different sequence on the partially buried microcolumn compared to the one shown in Figure 2B for the square DRIE microcolumn. The alkanes were found to elute faster than the polar compounds. For example, on the partially buried microcolumn *n*-C_{12} elutes at 2.97 s compared to 1,6-dichlorohexane, which elutes at 3.36 s. However, on the square DRIE microcolumn 1,6-dichlorohexane elutes first at 2.86 s, while *n*-C_{12} elutes at 4.29 s.

DISCUSSION

The work here demonstrates that microfabricated partially buried columns result in a more close to theoretical separation performance compared to square DRIE microcolumns. The key to the better performance was creating a channel shape that resulted in lower stationary phase pooling, cleaner microchannel structure, and the lower-dispersion wall profile of the partially buried microcolumns.

We find that the 34 cm long partially buried microcolumn gives lower HETP and reduced HETP values compared to the square DRIE microcolumn. To compare, the lowest HETP and reduced HETP values of 0.39 mm and 6.02 were measured on the partially buried microcolumn compared to 0.66 mm and 6.73 on the square DRIE microcolumn. The large deviation of the square DRIE microcolumn from the theoretical prediction as compared to the partially buried microcolumn can be attributed to either phase non-uniformity or extra-column dispersion. We believe that the extra-column dispersion is constant between the two types of columns because care was taken to keep the connector lengths equal. Dispersion sources not accounted for in the theoretical predictions include the turns and the Nanoport connectors. The key to obtaining separation performance closer to theoretical prediction on the partially buried microcolumn is thus attributed to the uniform phase deposition compared to square DRIE microcolumn. Also, a 10 component mix separates much faster and with a higher resolution on the partially buried microcolumn than on the square DRIE microcolumn. The inlet pressure and microcolumn temperature necessary for the separation on the partially buried microcolumn were found to be lower, which reflects lower energy need than the square DRIE microcolumns. The alkane, *n*-C_{12} elution during 10 component mix separation was found to be faster on the partially buried microcolumn compared to the square DRIE microcolumns, which again indicates the partially buried microcolumns have thinner stationary phase on the channel walls. The elution order of

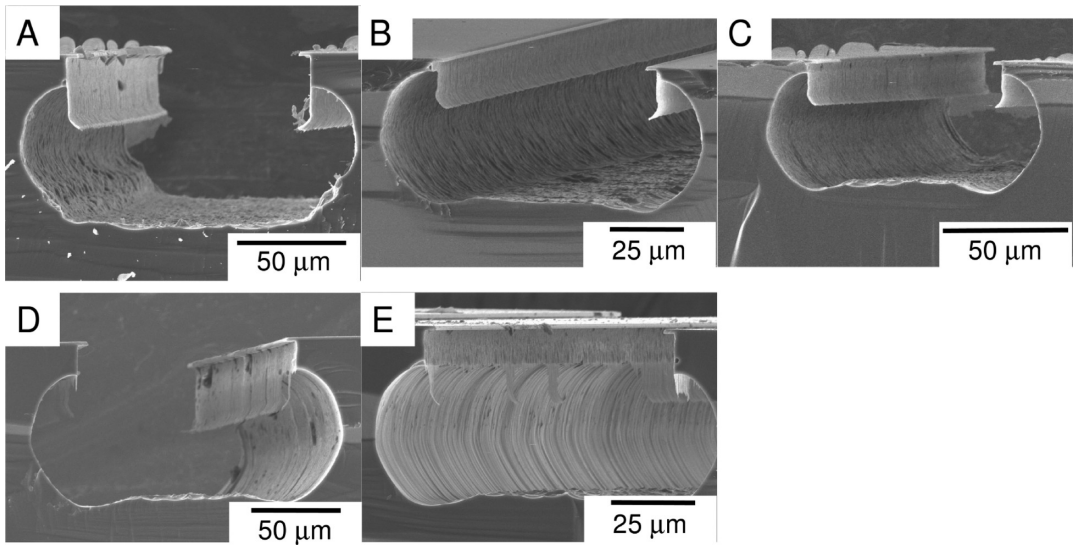

Figure 7. SEM image of partially buried microchannels showing the change in double-etched profile of the channel bottom as a function of RIE platen power during the iso-etch step; 25 W (A), 16 W (B), 12 W (C), 8 W (D), and 0 W (E). Process was carried out on a 5 mm × 10 mm wide test pieces.

compounds was found to be different on the two columns. It can be reasoned based on the familiar fact that elution orders are highly sensitive to changes in phase ratio and thermal separation conditions. The rise in the HETP value for the 34 cm long partially buried microcolumn above the optimum velocity is steeper than for a typical fused silica column, and this indicates the presence of severe extra-column band broadening arising from the Nanoport connectors. This leads to the underestimation of the performance of the partially buried microcolumns. Clearly there is a need for tighter integration of the microcolumns with other microfabricated GC components.

The two SF_6 based iso-etching steps included in the partially buried microcolumn fabrication method are responsible for the cleaner channel structures. The first iso-etch removes the micromasking defects that occur during the first DRIE step. The second iso-etch, which is comparatively a longer process eliminates any significant channel constrictions that may have been obtained because of mask damage, poisoned photoresist or particle defects.

The double-etched iso-tropic wall profile of the partially buried microcolumns was obtained in the first attempt of fabricating partially buried microcolumns, and no further process optimization was done to reduce the double-etched profile to simple iso-etch profile for the microcolumns. The dispersion in channels with double-etched wall profile has been modeled and discussed by Dutta and Leighton,[51−55] and they found that the double-etched iso-tropic wall profile lowers the Taylor−Aris dispersion because of the parabolic fluid velocity profile. However, the double-etched iso-tropic wall profile may not be the optimum wall profile for dynamically depositing stationary phases. We found that varying the ICP RIE platen power allows us to change the wall profile from double-etched to a simple iso-etch wall profile as shown in Figure 7. Results shown in Figure 7 were obtained on 5 mm × 10 mm patterned silicon pieces, and the findings do not directly translate to the ICP RIE platen power level for wafer-scale processing. However, the results show that it is feasible to change the channel shape and compare the performance of microcolumns with double-etched and simple isotropic wall profiles.

CONCLUSIONS

The results in this paper show that it is possible to a create silicon microcolumn with higher performance by creating a rounded channel wall profile for a microcolumn using the partially buried channel fabrication method. Minimum HETP of 0.39 mm was generated with the partially buried microcolumn compared to 0.66 mm obtained on the square DRIE microcolumn. The better performance may be attributed to the cleaner fabricated structures, lesser stationary phase pooling, and the double-etched isotropic wall profile of the partially buried microcolumns. A 10 component mix separation was obtained on the partially buried microcolumns at lower inlet pressures and column temperatures compared to DRIE microcolumn with a square wall profile. Also, the average peak width at half-maximum was much smaller for the partially buried microcolumn. Application of the findings of this work would render microcolumns that achieve faster and sharper separations in fast μGCs.

ACKNOWLEDGMENT

This work was supported financially by the Defense Advanced Research Projects Agency (DARPA) under U.S. Air Force Grant FA8650-04-1-7121. Any opinions, findings, and conclusions or recommendations expressed in this manuscript are those of the authors and do not necessarily reflect the views of the Defense Advanced Projects Research Agency, or the U.S. Air Force.

Received for review December 24, 2008. Accepted March 13, 2009.

AC8027382